Aerosol and Air Quality Research, 16: 930–942, 2016

ISSN: 1680-8584 print / 2071-1409 online
doi: 10.4209/aaqr.2015.08.0511

Interpretation of Atmospheric Aerosol Measurements by Means of a Numerical Simulator of New Particle Formation Events

Aare Luts*, Urmas Hõrrak, Jaan Salm, Marko Vana, Hannes Tammet

Institute of Physics, University of Tartu, Ülikooli 18, EE-50090, Tartu, Estonia

ABSTRACT

We performed a more comprehensive test of a new NPF parameter estimator published recently. The estimator considers measurements as test data and automatically adjusts the values of its physical control parameters according to the criterion of best fit. The parameters estimated within this procedure include nucleation rate, particle growth rate, birth size of nanoparticles etc. We analyzed all new particle formation events recorded during a measurement campaign at Hyytiälä, Finland. The results show a good performance in reproducing the time series of the concentrations of small air ions and aerosol nanoparticles in the diameter interval of 2.8–8.6 nm. The numerically estimated values of the parameters are in accordance with the results known from certain other studies carried out at Hyytiälä. We conclude the new method may appear useful in the analysis of several air ion and atmospheric aerosol measurements during new particle formation events.

Keywords: Atmospheric aerosols; Aerosol dynamics; Nanoparticle evolution model; Numerical simulation; Fitting to measurements.

INTRODUCTION

The phenomenon that a large number of charged atmospheric nanoparticles (intermediate ions) appear in the tropospheric air from time to time was discovered by air ion measurements at Tahkuse Observatory in 1985 (Tammet *et al*., 1987; Hõrrak *et al*., 1988; Tammet *et al*., 1988). About ten years later, the study of aerosol new particle formation (NPF) events spread over the world and nowadays the substantial role of these events in atmospheric aerosol generation is generally acknowledged (Weber *et al*., 1997; Hõrrak *et al*., 1998; Kulmala *et al*., 2004; Hirsikko *et al*., 2011; Nieminen *et al.*, 2014; Jayaratne *et al.*, 2015). Several different theories have been developed for the explanation of the NPF events. Nevertheless, the exact mechanisms of atmospheric nucleation are not yet completely known (Nieminen *et al*., 2011; Zhang *et al*., 2012; Kulmala *et al*., 2013; Leppä *et al*., 2013; Wang *et al*., 2013). A number of aerosol evolution models have been developed for solving different tasks. An overview and comparison of the models available up to 2003 was given by Korhonen *et al*. (2003). A later overview can be found in the introduction of a paper by Leppä *et al*. (2009).

The term "NPF" has a wide use and/or somewhat different meanings, but below we generally interpret it as the term "nucleation burst" used in the paper by Tammet and Kulmala (2005), where the authors introduced a new NPF simulation tool. The particular tool by Tammet and Kulmala is hereafter referred as "burst simulator" or "simulator". The tool simulates the evolution of small ions and the evolution of size distributions of neutral and charged nanometer particles. It does not consider the details of the mechanisms how the initial (thermodynamically stable) particles are formed. Therefore, in this simulator "nucleation burst" means just the evolution of the neutral and charged particles or nucleus that have already passed the size at which they become stable.

A wider and more complicated problem is the inverse modeling or the fitting of simulator output to the time series of certain parameters actually measured during nucleation events. This latter use of the simulation tool, i.e., the inverse modeling and automatic estimation of physical input parameters, was developed by us (Luts *et al.*, 2015). This new method, hereafter referred as "estimator", is applied also in the present study.

The simulator by Tammet and Kulmala (2005, 2007) is in several aspects similar to Ion-UHMA (Leppä *et al*., 2009) based on earlier models UHMA (Korhonen *et al*., 2004) and AEROION (Laakso *et al*., 2002). The main purpose of these models is to take a number of physical input parameters (ionization, nucleation and growth rates, etc.) and to yield the time- and size-dependent composition of neutral and

* Corresponding author.
Tel.: 372-7374774; Fax: 372-7375440
E-mail address: Aare.Luts@ut.ee

charged aerosol particles. The effective size region of the simulator by Tammet and Kulmala depends on input parameters. It can be up to 1000 nm, but commonly it follows the evolution and growth up to about 100 nm. Originally, the simulator considers the physical parameters (e.g., nucleation rate, particle growth rate) as the input and delivers selected output parameters (e.g., the time series of the particle size distribution) as a result. In actual research of atmospheric aerosols, the size distribution of particles is often directly measured and the above-mentioned physical parameters are subject to estimation on the basis of these measurements. One of the goals of the present paper is further testing the method by Luts *et al.* (2015) and estimation the values of the physical parameters that characterize the selected NPF events. Previously, this new method was tested by means of two NPF events measured at Hyytiälä in 2000. As demonstrated by Salm (2007) and Luts *et al.* (2015), a proper use of the burst simulator for the solution of inverse problem enables to estimate several essential parameters, which characterize the simulated NPF events (nucleation and growth rates, etc.). Still, so far the simulator was not intensively used and therefore, there is only little information on how well the simulator can reproduce the observed NPF events. In case the estimation results in reasonable values of the nucleation process characteristics, the burst simulator together with the optimization procedure can be extensively used to evaluate several essential characteristics of the NPF events (nucleation and growth rates, birth size of nanoparticles, etc.) not measured directly.

The specific goals of the present study are as follows:

1. To carry out a more comprehensive test of our estimator that helps to automate the simulations and to estimate the input parameters of the burst simulator by the criterion of the best similarity of the simulated output parameters to the corresponding measured parameters.
2. To find the estimated sets of the selected parameters for all the cases of NPF events recorded during a measurement campaign at Hyytiälä from 29 March to 9 April 2000.
3. To analyze the obtained results and also to study the charging state of the nanoparticles and the problems concerning ionization rate.

MEASUREMENTS AND METHODS

Measurement Site, Instrumentation and Campaign

The site of the measurements was the SMEAR II station, Hyytiälä, Southern Finland (61°51'N, 24°17'E, 180 m above sea level) (Hari and Kulmala 2005). The instrumentation and certain results from this measurement campaign have been published earlier (Mäkelä *et al.*, 2003; Luts *et al.*, 2015). A distinctive feature of this campaign was using two identical differential mobility particle sizers (DMPS) both measuring the aerosol particle size distribution in the range of 2.8–500 nm but with different pre-charging conditions. One of these DMPSs operated in the customary mode: the aerosol particles were charged in a bipolar charger (or neutralizer). The other DMPS was identical, but without the charger; thus it measured only naturally charged aerosol particles. In both DMPSs, negatively charged particles were analyzed according to their mobility by means of differential mobility analyzers (DMA). Later, this apparatus was modified and called Ion-DMPS (Gagné *et al.*, 2008). The concentrations of negative cluster ions were obtained by the method introduced by Tammet (1970) and using the raw data measured simultaneously by two integral air ion counters UT8401 designed and built at the University of Tartu.

The main measurement campaign lasted from 29 March to 14 April 2000, when the maximum number of instruments was operating. According to the classification introduced by Dal Maso *et al*. (2005), class 1a, 1b, or class 2 nucleation events of aerosol particles occurred on 7 days. In the present study we carry out the inverse modeling (optimization of the parameters that characterize the NPF events) for all these events and analyze the results for all these 7 days.

Method for the Estimation of NPF Parameters

Our original method (or estimator) for automated estimation of the physical parameters controlling aerosol NPF is described in (Luts *et al.*, 2015). It contains a previously published burst simulator (Tammet and Kulmala, 2005, 2007). The new method estimates the physical input parameters by recurrent simulations according to the criterion of best fit of the simulated output parameters with the known data. In principle this method can use any burst simulator provided the running of it can be automated, not only the simulator by Tammet and Kulmala (2005, 2007).

The simulator introduced by Tammet and Kulmala (2005, 2007) has 61 physical input parameters. Twelve parameters can have dual values: for free air and for forest environment. Technically, the simulator works as follows: initial numerical values are assigned to the parameters (also called input values or input parameters). Values for certain input parameters can be available from measurements, the initial values of some others can be estimated according to a priori available information. The values of estimated parameters can be more or less constrained, due to the reason that we either know or presume the range where these values are allowed to vary. The calculation will then result in a time-dependent set (or a time series) of the values of selected output parameters. For example, the output parameters can contain the time series of mobility-size distribution of nanoparticles and the concentration of cluster ions.

Our estimator compares the simulated output parameters with the results obtained by measurements. At the initial input parameters, the simulated output can be quite different from the results by measurements. If the similarity is not sufficient, then the values of selected physical input parameters are properly varied, and the next simulation trial is started etc., in order to reach a sufficient similarity between simulated and measured data. A proper organization of such a recurrent sequence of simulation trials is the essence of our estimator. The details of this method are described in (Luts *et al.*, 2015); general flowchart of the estimation algorithm is also presented in Supplement, Fig. S1. Supplement also contains certain comments about this flowchart. During numerous individual simulations within estimations, the computer programs technically never failed, which proves the stability of the algorithms.

Main Characteristics of the NPF Events

During the measurement campaign, NPF events occurred on 7 days. They belong to classes 1a, 1b, and 2, according to the classification by Dal Maso *et al*. (2005). General information about the events is given in Table 1. The meteorological and the detailed background aerosol parameters are presented in Supplement, Tables S1–S7.

The onset time of a burst cannot be absolutely exactly determined because commonly there is no abrupt and rapid jump in the concentrations of nanoparticles. To establish the onset time, we primarily selected the time point, when a visually considerable and persistent rise in the concentrations of the charged nanoparticles in a diameter range of 2.8–8.6 nm began. Fig. 1 depicts an example of measured time series. As seen in the figure, a considerable rise in the concentrations of both “natural" and "bipolar" ions (charged nanoparticles between 2.8 and 8.6 nm) started at about 9:00, but this point still cannot be considered as the proper onset time. A burst should start from sizes of about 1 nm (Kulmala *et al.* 2013), but the low end of our data (DMPS particle diameter) was 2.8 nm. Therefore the fresh particles generated at the onset of the burst could not be detected at 1 nm; they primarily had to grow up to 2.8 nm. In case we take the growth rate of nanoparticles for this size region to be between 1 and 2 nm h^{-1} (as found by Kulmala *et al.* 2013), we can assume an about 1 hour earlier burst onset time valid for about 1 nm size particles. The onset time values presented in Table 1 are established according to the abovementioned considerations. All the results of this paper presume just these burst onset times.

Parameters and Constraints Used in the Estimations

The problems related to the selected parameters, prior information and parameter constraints were discussed in (Luts *et al.*, 2015) already. Here we will present a brief overview and few comments about this topic.

Similarly to our previous paper, the estimation process is controlled by four parameters: by the concentrations of 1) negative and 2) positive small ions; by the integral concentrations of 3) the negatively charged nanoparticles within the size range 2.8–8.6 nm and 4) the neutral nanoparticles within the same range. The concentrations of

Table 1. General data about the considered NPF events at Hyytiälä in 2000. LST is the local standard time of Hyytiälä. The burst class is determined according to (Dal Maso *et al*., 2005). Briefly, NPF class 1a is characterized by prominent and clear shape and the corresponding parameters like growth rate can be (easily) derived. Class 1b is in some measure similar but the corresponding parameters are more ambiguous. In the case of class 2 the burst certainly happens but the corresponding parameters cannot be (directly) derived. Air mass origin is determined by our additional study of air mass trajectories by the SILAM model of atmospheric composition and dispersion (http://silam.fmi.fi/). N_{max} is the maximum number concentration of aerosol particles recorded by DMPS in the size range from 2.8 to 500 nm.

Date	Onset LST	Duration min	Class	Air mass origin	N_{max} cm^{-3}
29.03.	08:30	540	1b	Arctic	27200
30.03.	08:00	690	2	N-Atlantic	10200
2.04.	10:00	600	1b	Arctic	5800
6.04.	10:00	540	1b	Arctic	4800
7.04.	07:00	570	1a	Arctic	7600
8.04.	08:00	390	2	Arctic	16200
9.04.	07:30	510	1b	Arctic	8300

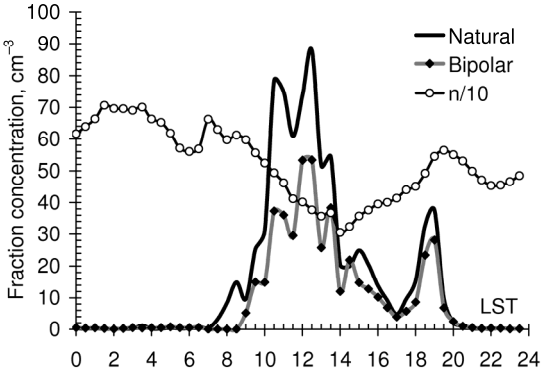

Fig. 1. Diurnal evolution of the particular number concentrations (cm^{-3}). Figure depicts the evolution of negatively charged aerosol particles and negative small ions at SMEAR II Station, Hyytiälä, Finland, on 8 April 2000. “Natural” denotes naturally charged particles in a diameter range of 2.8–8.6 nm, “Bipolar” denotes particles in the same size range charged in the bipolar charger, and “n” cluster air ions measured by means of air ion counters. “Fraction concentration” is the total number concentration within the particular size range (between 2.8 and 8.6 nm for “natural” and “bipolar” ions, below about 1.9 nm for cluster ions). LST is the local standard time (standard time for Finland or UTC + 2 hours).

negatively charged nanoparticles and negative cluster ions were directly measured. The summary concentration of neutral nanoparticles within the same size range was calculated using the measured data of bipolar charged (or neutralized) particles. The particular algorithm of these calculations is presented in Supplement, Appendix S1. Detailed results of these calculations (as an example) are in Supplement, Table S8. The concentration of positive cluster ions was not measured. However, several arguments support the statement that the concentrations of positive and negative cluster ions are strongly correlated and (roughly) $n+ = 1.1 \cdot n-$, where n+ and n– refer to the concentration of positive and negative cluster ions, respectively. The factor 1.1 is based on the long-term measurements at Tahkuse Observatory (Hõrrak *et al*., 2000).

By default, we can estimate (look for the optimal values of) all the 61 physical input parameters of simulator and the estimation algorithm can freely vary these input parameters. Still, several parameters are known from the measurements (e.g., the meteorological ones), these parameters are fixed at the measured values. Several parameters are known elsewhere. Recombination coefficient of cluster ions was assumed to be equal to $1.6 \cdot 10^{-6}$ cm^{-3} s^{-1}. Certain microphysical parameters, which determine the collision interaction between molecules, ions and particles as explained by Tammet and Kulmala (2005) were also fixed, likewise certain parameters of conifer forest. As a result we estimated 39 free physical parameters. Further details are available in (Luts *et al.*, 2015) and also in Supplement.

The number of known values employed as the basis of best fit of the simulated output parameters with the known data depends on particular case (on particular day). The estimated parameters (in the present study: 39 parameters) are valid for the whole case (in the present study: for the whole particular day). The number of known values depends on the number of time points within the particular time series and each time point contains four known values listed above. In this study, the minimum number of the time points within a series is 13 (on April 8), therefore this case is characterized by $4 \times 13 = 52$ known values (these values are listed in Table S6b). In addition to these (e.g., 52) values all cases also have 8 known values, listed in Tables S1a–S7a. Therefore, in the present study the 39 parameters are estimated using at least $52 + 8 = 60$ known values.

The burst simulator is sensitive to the values of ionization rates. In our previous paper we set the constraint that the ionization rates cannot be below 4.0 cm^{-3} s^{-1}, details in (Luts *et al.*, 2015) and also in Supplement. In this study we implemented the estimation provided the ionization rates are free.

Uncertainty of the estimated values cannot be strictly determined, because of complexity of the burst simulator. Nevertheless, the papers by Tammet and Kulmala (2005, 2007) contain certain theoretical considerations that result in plausible values of several model-dependent parameters. Reliability of the estimated values can be assessed by comparison of these values with the ones, either directly measured or known elsewhere. Such a comparison is accomplished below. Uncertainty of the estimated values can be assessed by running the method at several (slightly) different initial data and by intercomparison of the results, obtained by this manner. The results of such computational experiments are also summarized below.

RESULTS AND DISCUSSION

Summary of the New Results

As a result of estimation, optimal values of 39 input parameters have been obtained for all NPF events. Main parameters are presented in corresponding diagrams and tables (Fig. 2; Table 2(a)). Fig. 2 demonstrates that the shape, width and height of the time evolution curves obtained for charged and neutral particles in the diameter interval of 2.8–8.6 nm are comparable with those of the measured curves. Small fluctuating deviations of the simulated curves from the measured ones cannot be considered a serious shortcoming because simulator cannot take into account the fluctuations in the concentration of aerosol particles due to atmospheric non-homogeneity and turbulent fluctuations. As a result, the simulated curves cannot exactly match the measured curves. Table 3 contains specific results that belong to the discussion about the charging state of the particles.

Ionization Rate

As a result of the simulations, we obtained altogether 42 values of the ionization rate, 6 values for every particular NPF event day. For each day, we obtained the initial, halftime and final values for free air and the same three values for forest environment. The obtained values extend from 2.36 to 17.3 cm^{-3} s^{-1} with the average value of 5.0 cm^{-3} s^{-1} (Table 2(a)). The ionization rate appeared to be roughly equal in free air and inside the forest (average values of the ionization rate are 5.2 and 4.8 cm^{-3} s^{-1}, respectively). Previous studies have shown that ion production rate at Hyytiälä, calculated by external radiation and ^{222}Rn content, varied between 4.2 and 17.6 cm^{-3} s^{-1} while the lowest values were observed in spring (Hirsikko *et al*., 2007; Franchin, 2009). Our measurements were also in spring; until 9 April 2000 the soil was still frozen, and therefore, the low values of ionization rate can be possible.

Laakso *et al.* (2004) studied the period 20 March–11 April 2003 of the measurements at Hyytiälä. They found that the average ion production rate calculated from aerosol particle size distribution and air ion mobility distribution measurements was 2.6 cm^{-3} s^{-1} and the one based on external radiation and radon measurements was 4.5 cm^{-3} s^{-1}. The authors discussed several factors that could lead to the relatively low ionization rate values. Tammet *et al.* (2006) presented the probable reasons of such low ionization rates to occur due to (1) underestimation of small ion sink (2) the effect of cluster ion deposition inside the forest canopy and (3) aerosol hygroscopic properties. Hõrrak *et al.* (2005, 2008) thoroughly analyzed the measurements performed at Hyytiälä during the BIOFOR III campaign in 1999. The preliminary average ionization rate of about 3.3 ion pair cm^{-3} s^{-1}, calculated from the small ion balance equation applying the experimental data of aerosol particle size distribution and small ion concentration measurements,

was too small for continental stations because terrestrial ionization should originate from several concurrent agents(more effective agents than in marine environments) and the total ionization should exceed this value. Corrected values, taking into account additional sink of ions inside the forest and hygroscopic growth correction of particle sizes, were found to be about 2 times higher, about 6.3 ion pair cm^{-3} s^{-1}. Schobesberger *et al.* (2009) analyzed ionization

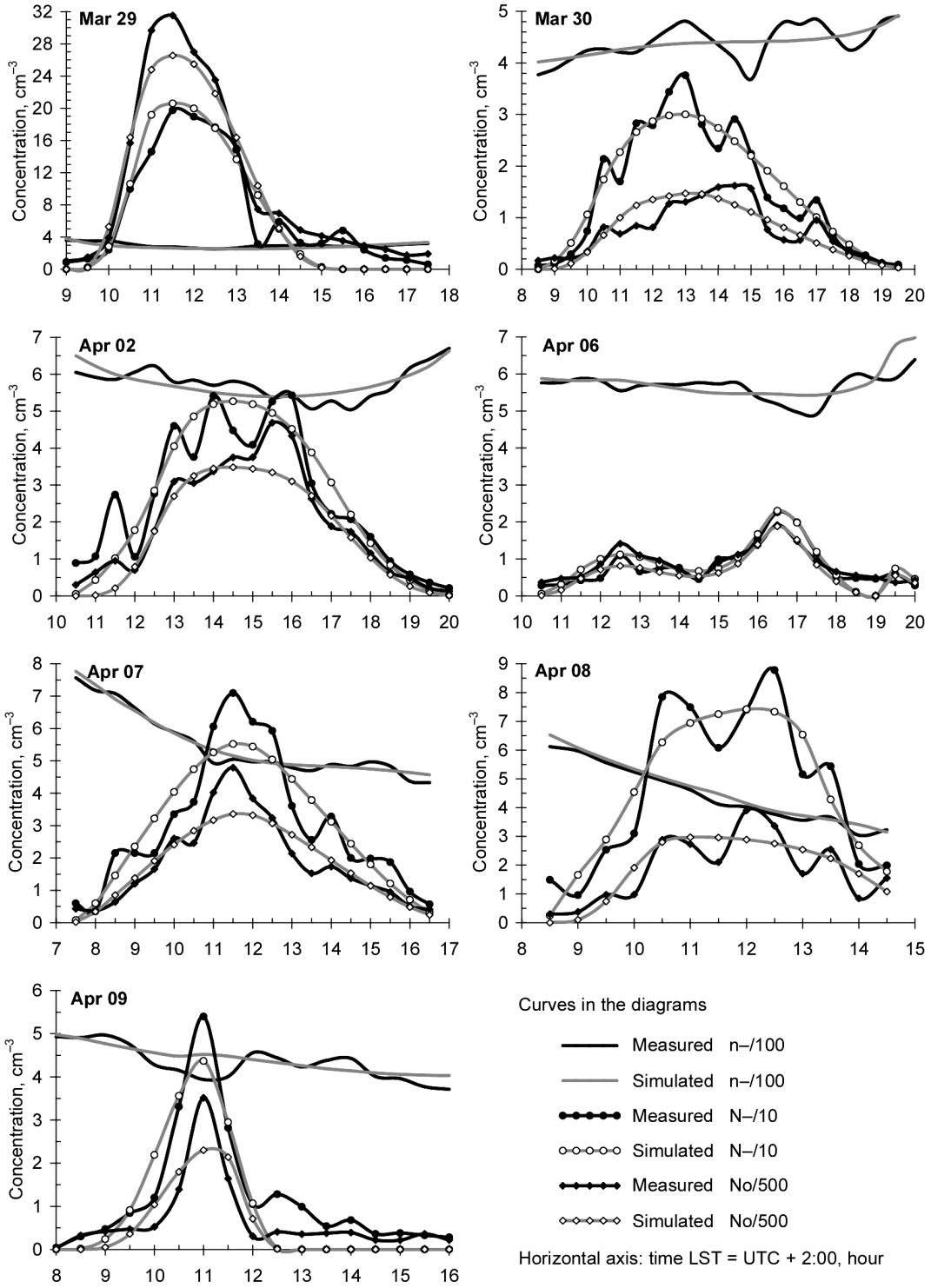

Fig. 2. Measured and simulated fraction concentrations of charged and neutral aerosol particles and of cluster ions at Hyytiälä in 2000. n– is the concentration of negative cluster ions, N– and No are the concentrations of negative, and neutral particles in the diameter interval of 2.8–8.6 nm. To draw the lines presented in the figure, the numerical concentrations are divided by the factors as given in the legend. Black lines represent the measured values and gray lines the simulations. Time on the x-axis is the local standard time (standard time for Finland or UTC + 2 hours).

Table 2(a). Results of the inverse solution of the NPF events recorded at SMEAR II Station, Hyytiälä. The values of measured parameters are given in Tables S1–S7 and not listed here. The mark (*) at particular parameter means that this parameter value is fixed (the estimator cannot modify this parameter). "IR" means "ionization rate", "NR" means "nucleation rate". Several parameters are given by the estimated initial, midpoint and final values. The actual values of these parameters at particular time points in the simulation interval are set inside the burst simulator, according to the selected approximation function, details in Supplement. In Tammet and Kulmala (2005, 2007) "midpoint" is referred as "halftime". Nucleation rates are given by their maximal values. The actual values of nucleation rate at particular time points in the simulation interval are set inside the burst simulator, according to the rules determined by the next 3 parameters (rise time of nucleation activity etc.). The model contains two condensing substances. The growth rates listed below are Knudsen growth rates and GR1 corresponds to the first substance and GR2 to the second substance. Details of the parameters are given in (Tammet and Kulmala, 2005, 2007) and summarized in Supplement.

Parameter name	29 March	30 March	2 April	6 April	7 April	8 April	9 April
Duration of NPF (min) (*)	540	690	600	540	570	390	510
Initial IR in free/in forest (cm^{-3} s^{-1})	4.0/4.0	4.0/4.0	3.0/4.0	5.4/4.0	4.6/4.0	6.8/4.6	4.5/3.6
Midpoint IR, in free air/in forest	3.8/5.1	3.6/4.6	5.0/4.0	4.7/4.6	4.0/4.0	4.0/4.0	3.5/3.8
Final IR in free air/in forest	17.3/8.5	5.1/4.6	6.0/6.6	7.0/7.1	4.9/5.6	4.9/4.6	2.4/5.8
Max NR + ions, free/forest (cm^{-3} s^{-1})	0.003/0.003	0.09/0.08	0.05/0.06	0.05/0.05	0.06/0.06	0.055/0.054	0.008/0.12
Max NR for – ions, free air/ forest	0.003/0.003	0.09/0.08	0.09/0.07	0.07/0.18	0.055/0.09	0.19/0.12	0.1/0.12
Max NR for neutrals, free/forest	8.3/8.0	1.0/2.0	0.6/1.6	0.7/2.0	0.6/1.1	0.7/1.6	1.3/1.5
Rise time of nucleation activity (min)	78	108	108	80	215	44	178
Steady nucleation activity (min)	25	128	128	200	17	217	1
Dropping nucleation activity (min)	231	366	255	204	296	55	33
Initial GR1, free/forest (nm h^{-1})	0.7/3.0	1.7/2.0	1.2/2.3	7.5/8.0	3.8/3.4	1.0/2.3	0.4/3.0
Midpoint GR1 in free/in forest	3.2/3.9	2.2/2.0	1.4/9.6	0.77/0.5	2.7/4.0	1.8/6.4	3.5/3.9
Final Knudsen GR1, free/forest	2.0/2.0	1.47/1.74	1.7/1.7	8.0/8.0	1.66/2.7	1.73/1.74	5.6/2.0
Density of first growth units (g cm^{-3})	3.4	2.2	2.0	2.0	1.5	2.0	2.0
Diameter of first growth unit (nm)	0.53	0.49	0.55	0.61	0.58	0.49	0.55
Initial GR2 free/forest (nm h^{-1})	2.5/3.0	3.0/3.0	3.3/2.7	2.0/2.0	6.5/2.5	2.9/2.7	2.8/3.0
Midpoint GR2 free/forest	2.0/4.0	2.2/3.0	2.9/3.2	8.0/8.0	1.7/2.5	2.7/2.7	2.7/4.0
Final Knudsen GR2, free/forest	2.0/2.0	3.0/3.0	1.3/2.9	4.0/4.0	6.4/3.0	1.3/2.9	2.0/2.0
Diameter of GR2 growth unit (nm)	0.6	0.49	0.49	0.6	0.6	0.49	0.6
GR2 condensation start diameter (nm)	2.1	2.0	2.0	2.0	2.4	1.65	2.0
Air residence distance in forest (m)	120	812	812	628	244	770	364
Birth size of particles (nm)	1.05	0.95	0.95	0.89	1.0	0.95	0.94
Initial wind speed in the forest (m s^{-1})	1.8	2.0	0.7	1.7	3.7	1.2	6.7
Midpoint wind in the forest (m s^{-1})	4.7	2.5	1.4	2.0	1.2	1.4	1.3
Final wind speed in the forest (m s^{-1})	1.8	0.6	0.3	0.6	0.7	1.5	2.3
Mobility of + small ions (cm^2 V^{-1} s^{-1})	1.33	1.19	1.4	1.49	1.37	1.4	1.37
Mobility of – small ions (cm^2 V^{-1} s^{-1})	1.52	1.32	1.55	1.65	1.52	1.55	1.54

rates at Hyytiälä, Finland, for the time period from March to December 2008. An average ion production rate of 3.3 ion pairs cm^{-3} s^{-1} was found, along with a significant monthly variation showing a maximum in summer and a minimum in winter.

The optimization process of this study sometimes resulted in the low values of ionization rate close to the values reported by Laakso *et al.* (2004), Hõrrak *et al.* (2008) and Schobesberger *et al*. (2009), but several studies have presented suggestive arguments that low ionization rates probably underestimate the small ion sink, these arguments support the conclusion that a correct ionization rate should be higher (Tammet *et al.*, 2006; Hirsikko *et al.*, 2007; Franchin, 2009). In our previous study, we set the low limit equal to 4 cm^{-3} s^{-1}, which resulted in values from 4.0 to 14.2 cm^{-3} s^{-1} with the average value of 4.9 cm^{-3} s^{-1}. Now we removed this constraint and ionization rate could freely vary within estimation process but the results are very close to the previous ones: previously the average value was 4.9 cm^{-3} s^{-1}, now it is 5.0 cm^{-3} s^{-1}. However, the problem of correct ionization rates seems to be still unsolved and needs some further study in the future.

The estimated mobility values of cluster ions are in average 1.36 cm^2 V^{-1} s^{-1} for positive ions and 1.52 cm^2 V^{-1} s^{-1} for negative ions. Such values are close to the ones known from the long-term measurements at Tahkuse Observatory (Hõrrak *et al*., 2000).

Birth Size of Particles

Within the simulator, this parameter is essentially linked to the nucleation rate; the latter parameter is discussed in the next section. All fresh particles become into existence with a certain birth size and at a certain nucleation rate. The birth size of particles is one important parameter that has not yet been thoroughly studied. The estimated value of this parameter appeared to be as small as 0.96 nm, on

average (Table 2(a)). Additional calculations by varying the birth size showed that the model is very sensitive in this respect. Even small variations by 3% gave rise to drastic changes in simulated graphs. Formally, moderate variations in the value of birth size can be compensated by large variations in the values of several other microphysical parameters of the burst simulator, first of all by large changes in the value of the extra temperature of quantum rebound (information about the quantum rebound can be found in Tammet and Kulmala (2005)). This implies that these parameters behave as correlated variables in our simulations. Neither birth size nor extra temperature can be directly measured, that is why these variations in our simulations are somewhat arbitrary. Still, such compensations are formally effective up to the values of the birth size of about 1.3 nm, even if we allow extremely large variations in the extra temperature. Above this value of birth size, the similarity between calculated and measured results lessens substantially. Provided the value of extra temperature is fixed, the values of birth size converge effectively and uniquely. If we try to compensate small variations in the birth size, unreasonably large variations in the extra temperature are needed. Therefore we preferred to fix the value of the extra temperature at the estimate by Tammet and Kulmala (2005, 2007), but considered the birth size as a free parameter.

It is known that from thermodynamic point of view the critical nucleus has a diameter on the order of 1 nm (Kulmala *et al*., 2007; Zhang *et al*., 2012). Kulmala *et al*. (2013) reported slightly larger values of 1.3–1.7 nm for mobility diameters. Our method yields the mass diameters. The problem of comparison of mass and mobility diameter values is not completely solved yet (Tammet, 2012). Broadly, our results are in agreement with the knowledge that a burst should start at about 1 nm.

Nucleation Rate

The nucleation rate is given by its top value. The actual value at a particular time moment within a simulation interval is determined by the parameters "rise time of nucleation activity", "time of steady nucleation activity", "time of dropping nucleation activity" (Table 2(a)). The effect of these parameters can be illustrated by few examples. On 7 April, nucleation rate increases slowly, has a constant maximal value for a short time, and decreases slowly. The NPF event on 8 April is characterized by a rapid increase and decrease in nucleation rate and by a long time while it has the top value meanwhile (Table 2(a), Fig. 2).

The estimated values of nucleation rate (or particle formation rate with the size equal to the "birth size") for charged particles are spread in the range from 0.003 to 0.19 cm^{-3} s^{-1}, and the rate for neutral particles from 0.56 to 8.3 cm^{-3} s^{-1} (Table 2(a)). The average values are 0.07 and 2.2 cm^{-3} s^{-1}, respectively. These outcomes are close to the results of several other studies. Dal Maso *et al*. (2005) analyzed the aerosol measurements at a boreal forest site at Hyytiälä, Finland, between 1996 and 2003. The mean appearance rate of larger than 3 nm particles was 0.8 cm^{-3} s^{-1}, varying from 0.06 to 5 cm^{-3} s^{-1}. Manninen *et al*. (2009) analyzed the measurements carried out during the EUCAARI field campaign at Hyytiälä in spring 2007. They estimated that the median formation rates of 2 nm total and charged particles were 0.65 cm^{-3} s^{-1} and 0.03 cm^{-3} s^{-1}, respectively. Gagné *et al.* (2012) measured aerosols by means of an Ion-DMPS in Helsinki, Finland between December 2008 and February 2010. The total particle formation rates in the 3–4 nm size range for class 1 particle formation events varied between 0.4 and 2.7 cm^{-3} s^{-1}. Vuollekoski *et al*. (2012) performed an analysis of a nucleation burst that was recorded at Hyytiälä on 1 April 2003. Different calculation methods gave the median formation rates of 3 nm particles 1.75 cm^{-3} s^{-1} and 1.13 cm^{-3} s^{-1}. Kulmala *et al*. (2013) reported that during the days with active aerosol formation, the maximum formation rate of 1.5-nm particles approached roughly 4 cm^{-3} s^{-1} around noon, while the same rate for charged particles was about 50 times lower.

Although our nucleation rate characterizes about 1 nm particles in diameter, the majority of the studies discussed above characterize the particles with sizes between 1.5 and 3 nm. The particles born with sizes of about 1 nm can vanish before they grow up to larger sizes. The survival percentage of 1 nm particles depends on several factors, primarily on growth rate and the parameters that determine the sink of the particles. Our evaluation demonstrated that at the conditions, characteristic for our cases, at least 50% of 1 nm particles should grow to about 3 nm. Therefore, the nucleation rates obtained elsewhere and summarized above, are still approximately comparable with the rates obtained in this study.

Growth Rate

The algorithm of the burst simulator includes two independent growth processes. The first process (GR1) is considered responsible for the initial slow growth of particles and simulates attachment of units of non-evaporating substance (e.g., sulphuric acid). The second one (GR2) simulates attachment of some evaporating substance (e.g., low volatile organic compounds) and is effective for the particles that have passed the threshold size of the nano-Köhler model. Technically the growth is implemented by adding (and/or evaporating) certain "growth units" described by diameters and densities (Table 2(a)). The growth unit is a molecule or cluster of condensing substance as explained by Tammet and Kulmala (2005). Both GR1 and GR2 are controlled by size-independent partial plain Knudsen growth rates corresponding to fictive sticky sizeless growth units of a specific substance. The actual (measurable) growth rates differ from the plain ones by specific size dependent factors; the values of the factors are usually between 1 and 1.5, see Tammet and Kulmala (2005).

The estimated values of the initial, midpoint and final rates for GR1 extend from 0.4 to 9.6 nm h^{-1} with the average value of 3.06 nm h^{-1}. GR2 values extend from 1.3 to 8.0 nm h^{-1} with the average value of 3.12 nm h^{-1} (Table 2(a)). The threshold size of the nano-Köhler model (i.e., the particle size at which GR2 becomes effective) has values from 1.65 to 2.4 nm. Diameters of the "growth units" are in average 0.54 and 0.55 nm for GR1 and GR2, respectively (Table 2(a)). Summary of certain former results derived

from previous numerous measurement campaigns carried out mainly at Hyytiälä, Finland is presented in Table 3. The corresponding textual overview is given in Supplement. We can conclude that the growth rate values estimated in this study are close to the ones, derived formerly from other measurements.

When to compare the estimated GR values with the classes of corresponding NPF events, the average GR values of the events assigned to the classes 1a and 1b is larger than the GR values of the events assigned to the class 2 (Table 2(b)). These average GR values are about 3.2 and 2.5 nm h^{-1}, respectively, and the difference of these values is statistically significant at the level of about 5%.

The estimated values of threshold size of the nano-Köhler model coincide well with the nano-Köhler threshold diameter of about 1.7 nm recently published by Kulmala *et al.* (2013). The "diameters of growth unit" together with polarizabilities could, in principle, help to identify the substances, responsible for GR1 and GR2. Many studies demonstrated that certain trace gases (besides sulphuric acid) could induce NPF. Both the specifics and the magnitude of the effect depend on the particular substance (e.g., Luts *et al.*, 2011a, b; Ortega *et al.*, 2012). We estimated the diameters of growth units, whereas polarizabilities are fixed. The estimated average values of the diameters for GR1 and GR2 are close to each other (0.54 and 0.55 nm, respectively). This information is clearly not sufficient to identify the substances but implies that 1) the growth units should not be very large molecules, and 2) the "units" responsible for GR2 should be slightly larger. When to compare the estimated growth unit diameter values with the classes of corresponding NPF events, the average diameter value of the events assigned to the classes 1a and 1b appears to be larger than the diameter value of the events assigned to the class 2 (about 0.58 and 0.49 nm, respectively), but the difference cannot be statistically proved because of the limited number of the values and large deviations. The same can be marked out for the values that characterize the diameter where the condensation GR2 starts. The corresponding average values are about 2.1 and 1.8 nm (Table 2(b)).

Small molecules (e.g., sulphuric acid) plausibly determine the first stages of growth, but at the later stages some larger molecules (e.g., various VOC molecules with masses above 300 Da) should become dominant (e.g., Kulmala *et al.*, 2013). According to the results by Ehn *et al.* (2011), a particle with mass about 300 Da should have a diameter of about 1.5 nm, far larger than 0.55 nm. Nevertheless, there is no standardized relationship between the mass and size; in the simulator by Tammet and Kulmala (2005) the particles with masses of 300 Da have diameters of about 0.8 nm, not about 1.5 nm. Therefore, the estimated diameters for GR1 (0.54 nm in average) can fit well for the first stages of the growth. Some hypothetical discrepancy within the diameters for GR2 can be caused by our test data, which are limited

Table 2(b). Results of the inverse solution of the NPF events recorded at SMEAR II Station, Hyytiälä (a copy of the ones from Table 2(a)), but organized in a way that facilitates the comparison of the results with the classes of corresponding NPF events. The classes are determined according to the classification by Dal Maso *et al*. (2005). Meaning of the terms "IR", "NR", "GR1" and "GR2" is equal to that in Table 2(a).

Parameter name	7 April	29 March	2 April	6 April	9 April	30 March	8 April
NPF class	1a	1b	1b	1b	1b	2	2
Average IR (cm^{-3} s^{-1})	4.8	5.6	4.8	5.0	4.6	4.5	4.7
Max NR + ions (cm^{-3} s^{-1})	0.06	0.003	0.06	0.05	0.12	0.09	0.055
Max NR for – ions	0.09	0.003	0.09	0.18	0.12	0.09	0.19
Max NR for neutrals	1.1	8.3	1.6	2.0	1.5	2.0	1.6
Average GR1 (nm h^{-1})	2.9	2.4	3.0	5.2	3.1	1.9	2.5
Average GR2 (nm h^{-1})	3.4	2.5	2.5	4.4	2.7	2.9	2.5
Diameter of GR2 growth unit (nm)	0.6	0.6	0.49	0.6	0.6	0.49	0.49
GR2 condensation start diameter (nm)	2.4	2.1	2.0	2.0	2.0	2.0	1.65
Birth size of particles (nm)	1.0	1.05	0.95	0.89	0.94	0.95	0.95
Charging state (%)	3.1	1.5	2.9	2.6	3.6	4.0	4.4
Mobility of + small ions (cm^2 V^{-1} s^{-1})	1.37	1.33	1.4	1.49	1.37	1.19	1.4
Mobility of – small ions (cm^2 V^{-1} s^{-1})	1.52	1.52	1.55	1.65	1.54	1.32	1.55

Table 3. Summary of the growth rates, obtained by certain former studies.

Publication, data origin	Size range, nm	GR, nm h^{-1}
Dal Maso *et al*. (2005), Hyytiälä	"Nucleation mode particles"	3.0
Hirsikko *et al*. (2005), Hyytiälä	1.3–3	1–2
	3–7	2–4
Manninen *et al*. (2009), Hyytiälä	3–7	3.8
Yli-Juuti *et al*. (2011), Hyytiälä	1.5–3	1.9
	3–7	3.8
Gagné *et al*. (2012), Helsinki	3–7	3.2–7.5
Vuollekoski *et al*. (2012), Hyytiälä	"Nanometer particles"	3.4

with the sizes of 8.6 nm. Due to this relatively low upper size, larger molecules could perhaps not take the full effect but the growth was still mainly controlled by the first substance.

Forest Parameters

For forest we estimated four free parameters: "air residence distance in forest" and wind speeds within forest at initial, midpoint and final time moments within simulation interval. The optimized "air residence distance in forest" ranged from 120 m to 812 m. Differences in this parameter value between the bursts can be caused by differences in forest and terrain features when the air mass approaches the measurement site from different directions, or by the changing wind speed. The forest features were not explicitly studied and therefore the estimated values cannot be accurately compared to the exact values known elsewhere. Broadly, such air residence distances seem plausible. The wind speed in the simulating tool by Tammet and Kulmala (2007) has a certain specific meaning: it rather characterizes an average wind speed in an extended forest massive than at a fixed geographical point. Initial, midpoint and final wind speed estimates are in the interval from 0.33 to 6.7 m s^{-1} with the mean of 1.9 m s^{-1}. These estimations cannot be correctly compared with the corresponding data obtained by measurements, because there is no such measured quantity available. Nevertheless, we can formally compare the estimated midpoint wind speeds to the ones measured around the noon on these days at the fixed routine measurement site of the SMEAR II station. The measured wind speeds were higher on 29 and 30 March, and on 6 April (1.7 m s^{-1} in average) and lower on other days (0.74 m s^{-1} in average). The simulated wind speeds are 3.1 m s^{-1} and 1.1 m s^{-1}, respectively. Thus the simulated values correlate to the measured ones, despite the fact that, in principle, the simulated values and the measured values have not exactly the same physical meanings.

Charging State

The burst simulator yields the concentrations of charged and neutral nanoparticles. These results allow drawing some conclusions also for the charging state, i.e., the extent by which the charged fraction of aerosol particles differs from the corresponding equilibrium charged fraction (Kerminen *et al*. 2007). Based on the results by Reischl *et al*. (1996) and Vana *et al*. (2006), the average percentage of negatively charged particles in the diameter interval 2.8–8.6 nm was estimated to be about 2.3% in steady state charge distribution, showing an increase from 1.1% to 4.6% within the size range 2.8–8.6 nm. The measurement range of DMPS begins at a diameter of 2.8 nm, but the growth of aerosol particles starts at about 1.0 nm. Thus the growth rate of particles is an especially significant parameter, when we try to assess the electrical state of nanoparticles. The charging steady state for nanoparticles in atmospheric air is attained in about 1 h (Hoppel *et al*., 1985). If the growth rate is too low, about 1 nm h^{-1} or lower, then the particles can attain the charging steady state before they will be measured by the DMPS. Moreover, as the neutralization rate of the charged particles exceeds by many orders of magnitude the charging rate of initially neutrally born particles, the particle populations tend to be undercharged more often than overcharged, compared to steady state.

Table 4 presents the percentages of charged fractions of nanoparticles, calculated as averages for a particular NPF event. The values are calculated from both measured data and simulated data. Comparison of these results to the equilibrium percentage (column "steady state %" in Table 4) discussed above yields a conclusion that on 30 March, 8 April and 9 April the particles seem to be overcharged whereas on 29 March they are undercharged. If the actual percentage of charged fraction is higher than the equilibrium percentage (here: 2.3%, as discussed above), the nucleation processes likely involve significant part of ions because charged new nanoparticles spring up more rapidly than usually. In case one wants to assess the part of ion-induced nucleation, comparison of actual parts of charged fractions with the steady-state part (2.3%) is critical. In the present study, the processes within NPF events at 30 March, 8 April and 9 April likely involve significant part of ion-induced nucleation. More in detail, Table 4 contains two columns

Table 4. Measured and simulated charged fractions of nanoparticles (%) at the SMEAR II station, Hyytiälä. Columns "charged %, meas" present the average values of charged fractions of negative nanoparticles, calculated from measured data and assuming that N– = N+. "Charged %, sim" present the average values of charged fractions of negative nanoparticles, calculated from modeled data. Columns "…(1)" contain the data at all-time points, columns "…(2)" contain only the data, where all "N–" and "No" are substantially above zero (at least 5% from the maximal value). Column "steady state" contains the average steady-state percentage of negatively charged particles in the diameter interval 2.8–8.6 nm, based on the results by Reischl *et al*. (1996) and Vana *et al*. (2006); this percentage can be used to assess nanoparticle overcharging and/or undercharging.

Day	charged %, meas (1)	charged %, meas (2)	charged %, sim (1)	charged %, sim (2)	steady state %
March 29	1.4	1.3	1.1	1.5	2.3
March 30	3.3	3.7	4.2	4.0	2.3
April 2	2.9	2.7	3.0	2.9	2.3
April 6	1.8	1.8	2.3	2.6	2.3
April 7	3.1	3.2	3.0	3.1	2.3
April 8	4.8	4.5	11.7	4.4	2.3
April 9	3.4	4.0	1.8	3.6	2.3
Average	2.9	3.0	3.9	3.2	2.3

for both measured and simulated data. The values in the first columns are the averages, taking into account the values at all the time points within a particular NPF event. The values in the second columns are also the averages, but take into account only the values that are above 5% from the maximal value within a particular NPF event. Detailed calculations for a particular NPF event are given in Supplement, Table S8.

According to the present simulations the charging state of the NPF events belonging to class 2 exceeds that of the other NPF events (new Table 2(b)). This result is already known formerly, e.g., by Vana *et al.* (2006). This result is another proof that our method is able to yield the correct estimates of the charging state values.

In summary we can conclude that the simulated percentages of the charged fraction are close to the ones, calculated from measured data. The largest inequality is in the values that describe the event at 6 April (1.8% from experimental results, 2.6% from simulated ones). This inequality is mainly *due to* the specific shape of the NPF event: this event has two maxima: the first at about 12:30 and the second at about 16:30. Unfortunately, current version of burst simulator cannot simulate such events very well because within simulator both nucleation and growth rates can have only one maximum within a particular simulated event. The general similarity of the results can be considered as another proof that the concentrations of charged and neutral nanoparticles obtained by simulations behave similarly to the ones, recorded by measurements and the simulated concentrations can be used to assess the charging state valid within a particular NPF event.

CONCLUSIONS

We implemented a more comprehensive test of our estimator that enables inverse modeling or the fitting of simulator output to the certain time series actually measured during NPF events.

The estimator includes burst simulator by Tammet and Kulmala (2005, 2007). By the estimator we obtained the optimal values of several physical input parameters that characterize the NPF events recorded during a measurement campaign at Hyytiälä, Finland, from 29 March to 9 April 2000 (ionization, nucleation and growth rates, etc.). The number of input parameters of the burst simulator is large and the formally optimal values of certain parameters can appear to be correlated with each other. This is caused by the inherent nature of the existing burst simulator, not by our new algorithms. For example, variations in the values of "birth size of particles" can be partly compensated by changes in certain microphysical parameters, e.g. the ones, characterizing quantum rebound. To decrease such ambiguities we fixed certain input parameters on the basis of available a priori information. Provided the constraints, the solution of the inverse problem reliably converged and at the estimated values of the 39 input parameters the simulated time-dependent curves are generally close to those obtained by direct measurements.

The estimated ionization rate varied from 2.36 to 17.3 cm^{-3} s^{-1} with the average value of 5.0 cm^{-3} s^{-1}. In our previous study we constrained ionization rate to the values above 4 $cm^{-3}s^{-1}$. Now ionization rate was free but mostly the estimated values are still above 4 cm^{-3} s^{-1}, estimated values below this limit appear rarely. This result is in agreement with common expectation that continental ionization rates should be significantly higher than those found for the marine environment (should be higher than about 2 cm^{-3} s^{-1}). However, the problem of uncommon relatively low ionization rates is beyond this particular method and needs further independent study. The nucleation rate for charged nanoparticles varied from 0.003 to 0.19 cm^{-3} s^{-1} and the rate for neutral particles from 0.56 to 8.3 cm^{-3} s^{-1}. The average birth size of new particles was estimated to be 0.96 nm in terms of the mass diameter. The estimates of the particle growth rate spread from 0.4 to 9.6 nm h^{-1} with the average value of 3.1 nm h^{-1}. The estimated percentage of charged particles was between 1.5 and 4.4% and was close to the one, calculated from measured data (between 1.3 and 4.5%). Therefore, the results of simulation/estimation can also be used to assess the charging state valid within a particular NPF event. Three NPF events were likely driven by ion-induced nucleation.

Abovementioned results found by means of the automatic estimation do not contradict the existing knowledge about the atmospheric aerosol at Hyytiälä SMEAR II station that is known from discussed previous publications. We conclude that our NPF parameter estimator appears to be a productive tool for the analysis of NPF. The future prospects include a statistical analysis of a large number of NPF events recorded during simultaneous atmospheric ion, aerosol, and meteorological measurements at different locations.

The estimator package by Luts *et al.* (2015) and further support is available by contacting the authors. The burst simulator program by Tammet and Kulmala (2005, 2007) (without the estimator software) is freely available on the web http://code.google.com/p/aerosol-genesis-simulator/downloads/list.

ACKNOWLEDGEMENTS

This work was supported by the Estonian Research Council Project IUT20-11 and by the European Regional Development Fund through the Environmental Conservation and Environmental Technology R&D Programme project BioAtmos (3.2.0802.11-0043). The authors thank Prof. Markku Kulmala and Prof. Jyrki Mäkelä for their support at the measurement campaign and for their useful comments at the preparation of this article. The authors also thank the staff of the SMEAR II station for the support in measurements.

SUPPLEMENTARY MATERIALS

Supplementary data associated with this article can be found in the online version at http://www.aaqr.org.

REFERENCES

Dal Maso M., Kulmala M., Riipinen I., Wagner R., Hussein T., Aalto P.P. and Lehtinen K.E.J. (2005).

Formation and Growth of Fresh Aerosols: Eight Years of Aerosol Size Distribution Data from SMEAR II, Hyytiälä, Finland. *Boreal Environ. Res.* 10: 323–336.

Ehn, M., Junninen, H., Schobesberger, S., Manninen, H.E, Franchin, A., Sipilä, M., Petäjä, T., Kerminen, V.M., Tammet, H., Mirme, A., Mirme, S., Hõrrak, U., Kulmala, M. and Worsnop, D.R. (2011). An Instrumental Comparison of Mobility and Mass Measurements of Atmospheric Small Ions. *Aerosol Sci. Technol.* 45: 522–532, doi: 10.1080/02786826.2010.547890.

Franchin, A. (2009). Relation between ^{222}Rn Concentration and Ion Production Rate in Boreal Forest. In *Proceedings of the Finnish Center of Excellence and Graduate School in "Physics, Chemistry, Biology and Meteorology of Atmospheric Composition and Climate Change" Annual Workshop 27.–29.4.2009*, Kulmala, M., Bäck, J., Nieminen, T. and Lauri, A. (Eds.), Report Series in Aerosol Science, 102, University of Helsinki Press, Helsinki, pp. 105–108

Gagné, S., Laakso, L., Petäjä, T., Kerminen, V.M. and Kulmala, M. (2008). Analysis of One Year of Ion-DMPS Data from the SMEAR II Station, Finland. *Tellus Ser. B* 60: 318–329.

Gagné, S., Leppä, J., Petäjä, T., McGrath, M.J., Vana, M., Kerminen, V.M., Laakso, L. and Kulmala, M. (2012). Aerosol Charging State at an Urban Site: New Analytical Approach and Implications for Ion-induced Nucleation. *Atmos. Chem. Phys.* 12: 4647–4666.

Hari, P. and Kulmala, M. (2005). Station for Measuring Ecosystem–Atmosphere Relations (SMEAR II). *Boreal Environ. Res.* 10: 315–322.

Hirsikko, A., Laakso, L., Hõrrak, U., Aalto, P.P., Kerminen, V.M. and Kulmala, M. (2005). Annual and Size Dependent Variation of Growth Rates and Ion Concentrations in Boreal Forest. *Boreal Environ. Res.* 10: 357–369.

Hirsikko, A., Paatero, J., Hatakka, J. and Kulmala, M. (2007). The ^{222}Rn Activity Concentration, External Radiation Dose and Air Ion Production Rates in a Boreal Forest in Finland between March 2000 and June 2006. *Boreal Environ. Res.* 12: 265–278.

Hirsikko, A., Nieminen, T., Gagné, S., Lehtipalo, K., Manninen, H.E., Ehn, M., Hõrrak, U., Kerminen, V.M., Laakso, L., McMurry, P.H., Mirme, A., Mirme, S., Petäjä, T., Tammet, H., Vakkari, V., Vana, M. and Kulmala, M. (2011). Atmospheric Ions and Nucleation: A Review of Observations. *Atmos. Chem. Phys.* 11: 767–798.

Hoppel ,W.A. (1985). Ion-Aerosol Attachement Coefficients, Ion Depletion, and the Charge Distribution on Aerosols. *J. Geophys. Res*. 90: 5917–5923.

Hõrrak, U., Tammet, H., Salm, J. and Iher, H. (1988). Diurnal and Annual Variations of Atmospheric Ionisation Quantities in Tahkuse. *Acta et Comm. Univ. Tartuensis* 824: 78–83 (in Russian, with English Summary).

Hõrrak, U., Salm, J. and Tammet, H. (1998). Bursts of Intermediate Ions in Atmospheric Air. *J. Geophys. Res.* 103: 13909–13915.

Hõrrak, U., Salm, J. and Tammet, H. (2000). Statistical Characterization of Air Ion Mobility Spectra of Tahkuse Observatory: Classification of Air Ions. *J. Geophys. Res*. 105: 9291–9302.

Hõrrak, U., Aalto, P.P., Salm, J., Mäkelä, J.M., Laakso, L. and Kulmala, M. (2005). Characterization of Air Ions in Boreal Forest Air during BIOFOR III Campaign. *Atmos. Chem. Phys. Discuss.* 5: 2749–2790.

Hõrrak, U., Aalto, P.P., Salm, J., Komsaare, K., Tammet, H., Mäkelä, J.M., Laakso, L. and Kulmala, M. (2008). Variation and Balance of Positive Air Ion Concentrations in a Boreal Forest. *Atmos. Chem. Phys.* 8: 655–675.

Jayaratne, E.R., Ling, X. and Morawska, L. (2015). Suppression of Cluster Ions during Rapidly Increasing Particle Number Concentration Events in the Environment. *Aerosol Air Qual. Res.* 15: 28–37.

Kerminen, V.M., Anttila, T., Petäjä, T., Laakso, L., Gagné, S., Lehtinen, K.E.J. and Kulmala, M. (2007). Charging State of the Atmospheric Nucleation Mode: Implications for Separating Neutral and Ion-induced Nucleation. *J. Geophys. Res*. 112: D21205.

Korhonen, H., Lehtinen, K.E.J., Pirjola, L., Napari, I., Vehkamäki, H., Noppel, M. and Kulmala, M. (2003). Simulation of Atmospheric Nucleation Mode: A Comparison of Nucleation Models and Size Distribution Representations. *J. Geophys. Res*. 108: 4471, doi: 10.1029/2002JD003305.

Korhonen, H., Lehtinen, K.E.J. and Kulmala, M. (2004). Multicomponent Aerosol Dynamics Model UHMA: Model Development and Validation. *Atmos. Chem. Phys.* 4: 757–771.

Kulmala, M., Vehkamäki, H., Petäjä, T., Dal Maso, M., Lauri, A., Kerminen, V.M., Birmili, W. and McMurry, P.H. (2004). Formation and Growth Rates of Ultrafine Atmospheric Particles: A Review of Observations. *J. Aerosol Sci*. 35: 143–176.

Kulmala, M., Riipinen, L., Sipilä, M., Manninen, H.E., Petäjä, T., Junninen, H., Dal Maso, M., Mordas, G., Mirme, A., Vana, M., Hirsikko, A., Laakso, L., Harrison, R., Hanson, L., Leung, C., Lehtinen, K.E.J. and Kerminen, V.M. (2007). Towards Direct Measurements of Atmospheric Nucleation. *Science* 318: 89–92.

Kulmala, M., Kontkanen, J., Junninen, H., Lehtipalo, K., Manninen, H.E., Nieminen, T., Petaja, T., Sipila, M., Schobesberger, S., Rantala, P., Franchin, A., Jokinen, T., Jarvinen, E., Aijala, M., Kangasluoma, J., Hakala, J., Aalto, P.P., Paasonen, P., Mikkila, J., Vanhanen, J., Aalto, J., Hakola, H., Makkonen, U., Ruuskanen, T., Mauldin, R.L., 3rd, Duplissy, J., Vehkamaki, H., Back, J., Kortelainen, A., Riipinen, I., Kurten, T., Johnston, M.V., Smith, J.N., Ehn, M., Mentel, T.F., Lehtinen, K.E., Laaksonen, A., Kerminen, V.M. and Worsnop, D.R. (2013). Direct Observations of Atmospheric Aerosol Nucleation. *Science* 339: 943–946.

Laakso, L., Mäkelä, J.M., Pirjola, L. and Kulmala, M. (2002). Model Studies on Ion-induced Nucleation in the Atmosphere. *J. Geophys. Res*. 107: 4427, doi: 10.1029/2002JD002140.

Laakso, L., Petäjä, T., Lehtinen, K.E.J., Kulmala, M., Paatero, J., Hõrrak, U., Tammet, H. and Joutsensaari, J. (2004). Ion Production Rate in a Boreal Forest Based on Ion, Particle and Radiation Measurements. *Atmos. Chem. Phys.* 4: 1933–1943.

Leppä, J., Kerminen, V.-M., Laakso, L., Korhonen, H., Lehtinen, K.E.J., Gagné, S., Manninen, H.E., Nieminen, T. and Kulmala, M. (2009). Ion-UHMA: A model for Simulating the Dynamics of Neutral and Charged Aerosol Particles. *Boreal Environ. Res.* 14: 559–575.

Leppä, J., Gagné, S., Laakso, L., Manninen, H.E., Lehtinen, K.E.J., Kulmala, M. and Kerminen, V.M. (2013). Using Measurements of the Aerosol Charging State in Determination of the Particle Growth Rate and the Proportion of Ion-induced Nucleation. *Atmos. Chem. Phys.* 13: 473–486.

Luts, A., Komsaare, K., Parts, T.E. and Hõrrak U. (2011a). Links between Two Different Types of Spectra of Charged Nanometer Aerosol Particles. *Atmos. Res.* 101: 527–538.

Luts, A., Parts, T.E., Hõrrak, U., Junninen, H. and Kulmala, M. (2011b). Composition of Negative Air Ions as a Function of Ion Age and Selected Trace Gases: Mass- and Mobility Distribution. *J. Aerosol Sci.* 42: 820–838.

Luts, A., Hõrrak, U., Salm, J., Vana, M. and Tammet, H. (2015). A Method for Automated Estimation of Parameters Controlling Aerosol New Particle Formation. *Aerosol Air Qual. Res.* 15: 1166–1177, doi: 10.4209/aaqr.2014.10.0232.

Manninen, H.E., Nieminen, T., Riipinen, I., Yli-Juuti, T., Gagné, S., Asmi, E., Aalto, P.P., Petäjä, P., Kerminen, V.M. and Kulmala, M. (2009). Charged and Total Particle Formation and Growth Rates during EUCAARI 2007 Campaign in Hyytiälä. *Atmos. Chem. Phys.* 9: 4077–4089.

Mäkelä J.M., Salm J., Smirnov V.V., Koponen I., Paatero J. and Pronin A.A. (2003). Measurements of the Mobility Distribution of Air Ions as a Source of Information for the Study of Aerosol Generation. In *Proceedings of 12th International Conference on Atmospheric Electricity, Vol. 2*, Chauzy, S. and Laroche, P. (Eds.), Versailles, France, 2003, pp. 793–796.

Nieminen, T., Paasonen, P., Manninen, H.E., Sellegri, K., Kerminen, V.M. and Kulmala, M. (2011). Parameterization of Ion-induced Nucleation Rates Based on Ambient Observations. *Atmos. Chem. Phys.* 11: 3393–3402.

Nieminen, T., Asmi, A., Dal Maso, M., Aalto, P.P., Keronen, P., Petäjä, T., Kulmala, M. and Kerminen, V.M. (2014). Trends in Atmospheric New-particle Formation: 16 Years of Observations in a Boreal-forest Environment. *Boreal Environ. Res.* 19: 191–214.

Ortega, I.K., Suni, T., Boy, M., Grönholm, T., Manninen, H.E., Nieminen, T., Ehn, M., Junninen, H., Hakola, H., Hellén, H., Valmari, T., Arvela, H., Zegelin, S., Hughes, T., Kitchen, M., Cleugh, H., Worsnop, D.R., Kulmala,, M. and Kerminen, V.M. (2012). New Insights into Nocturnal Nucleation. *Atmos. Chem. Phys*. 12: 4297–4312.

Reischl, G.P., Mäkelä, J.M., Karch, R. and Necid, J. (1996). Bipolar Charging of Ultrafine Particles in the Size Range below 10 nm. *J. Aerosol Sci.* 27: 931–949.

Salm, J. (2007). Simulation of an Aerosol Nucleation Burst. In *Nucleation and Atmospheric Aerosols*, O'Dowd, C.D. and Wagner, P.E. (Eds.), Springer, pp. 245–249.

Schobesberger, S., Franchin, A., Vana, M. and Kulmala, M. (2009). Analysis of the Ionization Rate at a Boreal Forest Measurement Site in Finland in 2008. In *Proceedings of the Finnish Center of Excellence and Graduate School in "Physics, Chemistry, Biology and Meteorology of Atmospheric Composition and Climate Change" Annual Workshop 27.–29.4.2009*, Kulmala, M., Bäck, J., Nieminen, T. and Lauri, A. (Eds.), Report Series in Aerosol Science, 102, University of Helsinki Press, Helsinki, pp. 386–389.

Tammet, H. (1970). The Aspiration Method for the Determination of Atmospheric Ion-spectra. IPST for NSF, Jerusalem, http://hdl.handle.net/10062/24240.

Tammet, H., Salm, J. and Iher, H. (1987). The Spectrum of Atmospheric Ions in the Range of 0.32–3.2 $cm^2/(V\ s)$. *Acta et Comm. Univ. Tartuensis* 755: 29–46 (in Russian, with English Summary).

Tammet, H., Salm, J. and Iher, H. (1988). Observation of Condensation on Small Air Ions in the Atmosphere. In *Atmospheric Aerosols and Nucleation. Lecture Notes in Physics*, Vol. 309, Springer, Vienna, pp. 239–240.

Tammet, H. and Kulmala, M. (2005). Simulation Tool for Atmospheric Aerosol Nucleation Bursts. *J. Aerosol Sci.* 36: 173–196.

Tammet, H., Hõrrak, U., Laakso, L. and Kulmala, M. (2006). Factors of Air Ion Balance in a Coniferous Forest according to Measurements in Hyytiälä, Finland. *Atmos. Chem. Phys.* 6: 3377–3390.

Tammet, H. and Kulmala, M. (2007). Simulating Aerosol Nucleation Bursts in a Coniferous Forest. *Boreal Environ. Res.* 12: 421–430.

Tammet, H. (2012). The Function-updated Millikan Model: A Tool for Nanometer Particle Size-mobility Conversions. *Aerosol Sci. Technol.* 46: i–iv, doi: 10.1080/02786826.2012.700740.

Vana, M., Tamm, E., Hõrrak, U., Mirme, A., Tammet, H., Laakso, L., Aalto, P.P. and Kulmala, M. (2006). Charging State of Atmospheric Nanoparticles during the Nucleation Burst Events. *Atmos. Res.* 82: 536–546.

Vuollekoski, H., Sihto, S.L., Kerminen, V.M., Kulmala, M. and Lehtinen, K.E.J. (2012). A Numerical Comparison of Different Methods for Determining the Particle Formation Rate. *Atmos. Chem. Phys.* 12: 2289–2295.

Wang, J., McGraw, R.L. and Kuang, C. (2013). Growth of Atmospheric Nano-particles by Heterogeneous Nucleation of Organic Vapor. *Atmos. Chem. Phys.* 13: 6523–6531.

Weber, R.J., Marti, J.J., McMurry, P.H., Eisele, F.L., Tanner, D.J. and Jefferson, A. (1997). Measurements of New Particle Formation and Ultrafine Particle Growth Rates at a Clean Continental Site. *J. Geophys. Res.* 102: 4375–4385.

Yli-Juuti, T., Nieminen, T., Hirsikko, A., Aalto, P.P., Asmi, E., Hõrrak, U., Manninen, H.E., Patokoski, J., Dal Maso, M., Petäjä, T., Rinne, J., Kulmala, M. and Riipinen, I. (2011). Growth Rates of Nucleation Mode Particles in Hyytiälä during 2003–2009: Variation with Particle Size, Season, Data Analysis Method and Ambient Conditions. *Atmos. Chem. Phys.* 11: 12865–12886.

Zhang, R., Khalizov, A., Wang, L., Hu, M. and Xu, W.

(2012). Nucleation and Growth of Nanoparticles in the Atmosphere. *Chem. Rev*. 112: 1957–2011.

Received for review, August 19, 2015
Revised, December 23, 2015
Accepted, February 1, 2016